Supporting Information

Ceria Promotion of Acetaldehyde Photo-oxidation in a TiO_2-based Catalyst: a Spectroscopic and Kinetic Study

Mario J. Muñoz-Batista, [a] María de los Milagros Ballari, [b] Alberto E. Cassano, [b] Orlando M. Alfano, [b,*] Anna Kubacka [a,*] Marcos Fernández-García [a]

[a] Instituto de Catálisis y Petroleoquímica, CSIC, C/Marie Curie 2, 28049-Madrid, Spain
[b] Instituto de Desarrollo Tecnológico para la Industria Química (INTEC, UNL-CONICET), Güemes 3450, 3000, Santa Fe, Argentina

1.- Photocatalytic measurements.

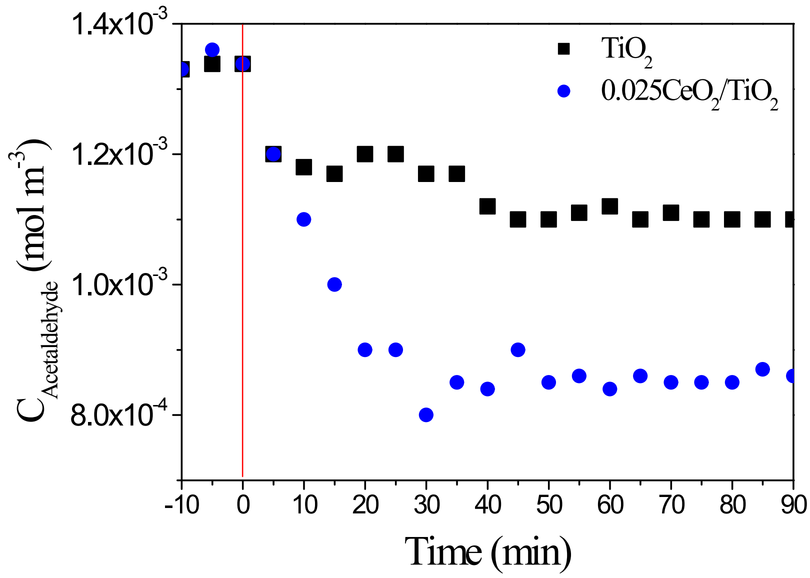

Fig. S1. Time evolution of the acetaldehyde conversion under visible irradiation. Co = 30 ppm, HR = 45 %; Irradiation level = 100%.

2.- External and Internal mass transfer

To determine if the external mass transfer resistance was significant, the modified Mear's criterion (C_M) was used (Eq. S1)

$$\frac{\langle r \rangle_{A_c} n}{k_c \langle C_b \rangle_V} < 0.1 \qquad S1$$

Where:

$$\langle r \rangle_{A_c} = \frac{Q\,(C_{out} - C_{in})}{m_c\,BET}$$

The influences of internal mass transfer were assessed by using the Weisz-Prater Criterion modified (Eq. S2).

$$\frac{\langle r \rangle_{A_c} r_{eq}^2}{D_{eff} C_s} < 1 \qquad S2$$

where:

$\langle r \rangle_{A_c}$: average reaction rate (mol m^{-2} s^{-1})

n: reaction order (assumed to be 1 for acetaldehyde)

k_c: mass transfer coefficient (m s^{-1})

$\langle C_b \rangle_V$: bulk average concentration (mol m^{-3})

Q: volumetric flow rate (m^3 s^{-1})

C_{out}: outlet concentration (mol m^3)

C_{in}: inlet concentration (mol m^3)

m_c: mass (g)

BET: BET surface area (m^2 g^{-1})

r_{eq}: equivalent radius (m)

C_s: film superficial concentration (mol m^{-3})

Table S1. Operating conditions of kinetic tests carried out in the study.

No.	Aceltadehyde Concentration (ppmv)	Irradiation Level[a] (%)	Relative humidity (%)
1	10	2	70
2	10	2	15
3	10	3	45
4	10	1	45
5	20	2	45
6	20	1	70
7	20	3	70
8	20	1	15
9	20	3	15
10	30	2	15
11	30	1	45
12	30	3	45
13	30	2	70

a) UV/Visible lamp intensity. Level 1: 9/35 %; level 2: 13/50 %; level 3: 25/100 %.

Table S2. C_M and C_{WP} for the 0.025CeO2-TiO_2 sample under UV and Visible light irradiation. Tests order and experimental conditions as mentioned in Table S1.

C_M		C_{WP}	
0.025CeO_2/TiO_2 UV	0.025CeO_2/TiO_2 Vis	0.025CeO_2/TiO_2 UV	0.025CeO_2/TiO_2 Vis
6.91E-04	2.85E-04	4.02E-08	1.83E-08
8.49E-04	3.66E-04	4.65E-08	2.28E-08
9.76E-04	5.89E-04	5.00E-08	3.58E-08
5.60E-04	2.08E-04	3.45E-08	1.37E-08
6.01E-04	2.33E-04	3.63E-08	1.52E-08
3.62E-04	1.01E-04	2.39E-08	6.85E-09
5.95E-04	2.90E-04	3.63E-08	1.90E-08
4.77E-04	2.09E-04	2.91E-08	1.37E-08
6.05E-04	2.59E-04	3.56E-08	1.67E-08
4.82E-04	1.94E-04	3.04E-08	1.29E-08
6.93E-04	4.13E-04	4.09E-08	2.66E-08
5.28E-04	1.48E-04	3.37E-08	9.89E-09
7.28E-04	3.86E-04	4.09E-08	2.43E-08

All experiments used to obtain the kinetic parameter satisfy the C_M/C_{WP} criteria. Note that, for the reaction under UV irradiation it was necessary to use irradiation levels lower than 25 %.

3.- Optical measurement results

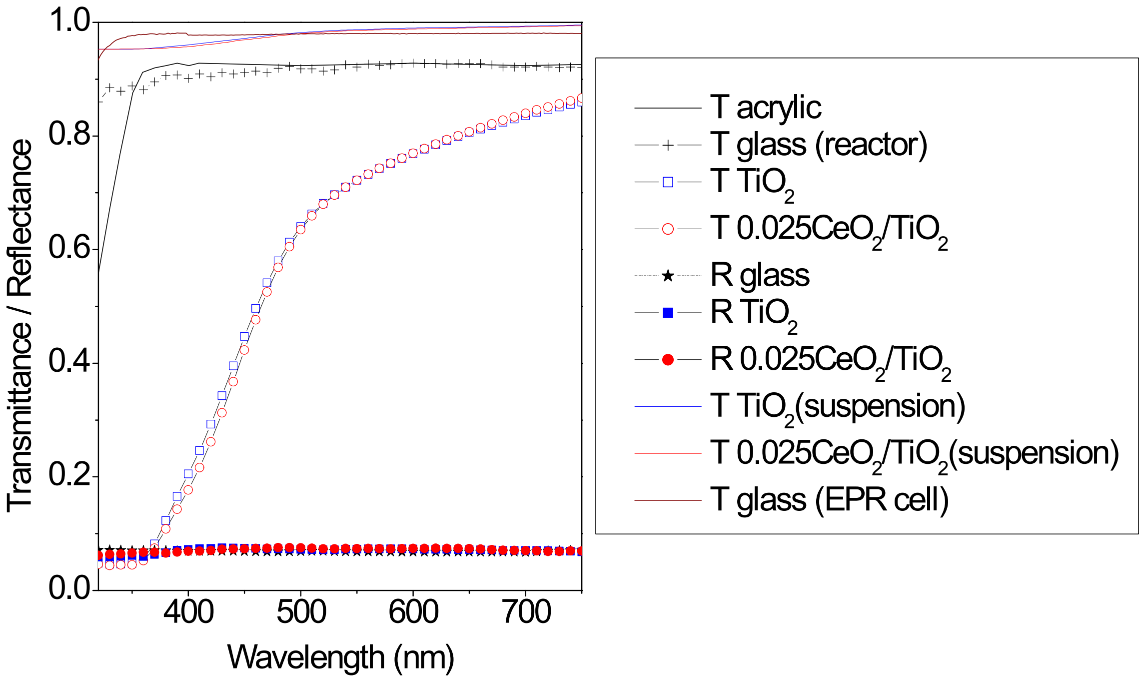

Fig. S2. (A) Transmittance (T) and reflectance (R) experimental values of the borosilicate plate, acrylic, and catalytic samples.

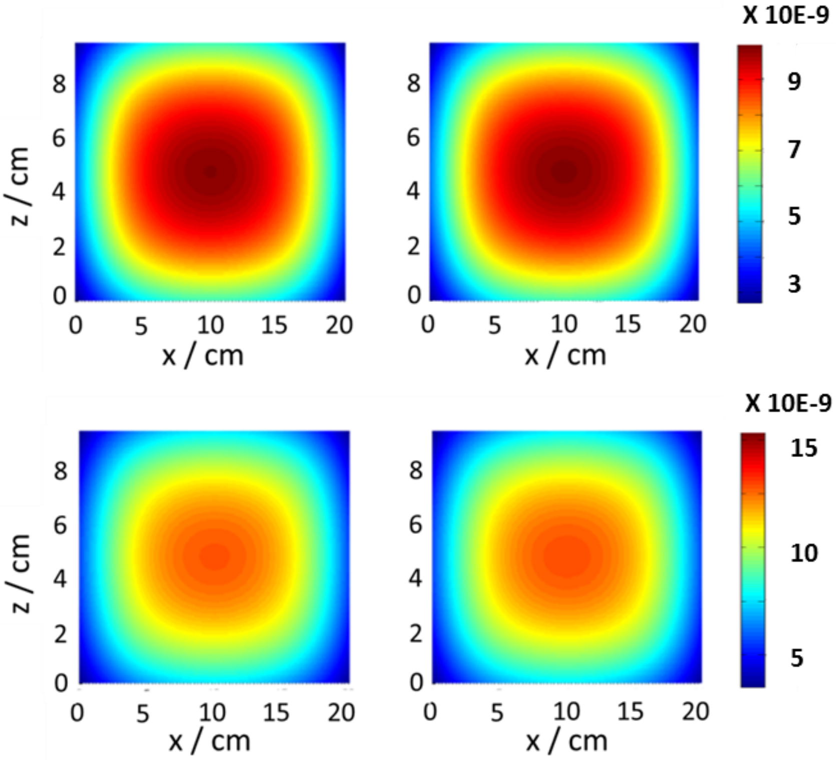

Fig. S3. Local superficial rate of photon absorption (Einstein cm^{-2} s^{-1}). Upper row: TiO_2 and $0.025CeO_2/TiO_2$ under UV irradiation. Lower row: TiO_2 and $0.025CeO_2/TiO_2$ under Visible irradiation.

Table S3. Local volumetric "EPR"-rate of photon absorption under UV and Visible irradiations.

Sample	UV $\langle e^{a,v} \rangle_V$ (Einstein cm^{-3} s^{-1})	Visible $\langle e^{a,v} \rangle_V$ (Einstein cm^{-3} s^{-1})
TiO_2	2.27×10^{-6}	2.24×10^{-6}
$0.025CeO_2/TiO_2$	2.29×10^{-6}	2.52×10^{-6}

4.- EPR Experimental details

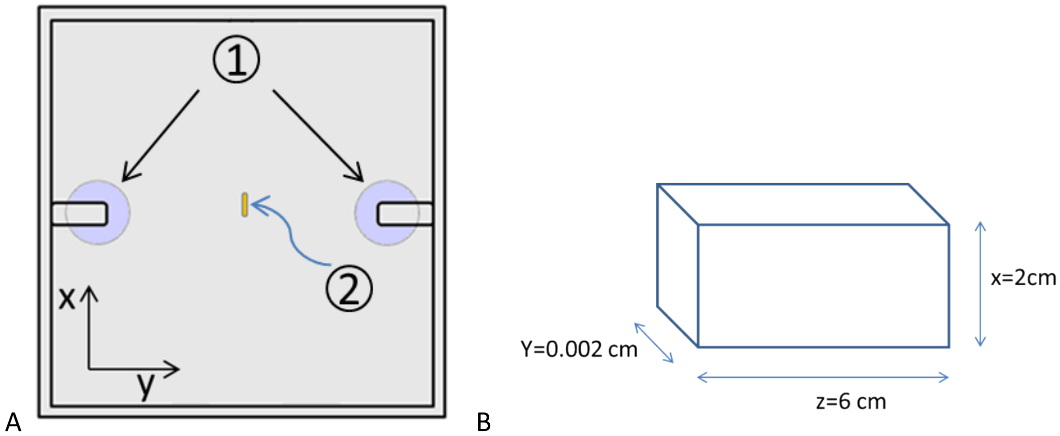

Fig. S4. (A) Side section view of the EPR reaction system. (1) Lamps, (2). EPR cell. (B) Scheme and dimension of the EPR cell.

5.- Integration Limits

5.1. Integration Limits of Eq. 18 of main text

$$\varphi_{mín} = \tan^{-1}\left(\frac{X_L - Xs}{Y_L}\right) - \sin^{-1}\left(\frac{R_L}{(X_L - Xs)^2 + (Y_L)^2}\right)$$

$$\varphi_{max} = \tan^{-1}\left(\frac{X_L - Xs}{Y_L}\right) + \sin^{-1}\left(\frac{R_L}{(X_L - Xs)^2 + (Y_L)^2}\right)$$

$$\Theta_{mín}(\varphi) = \cos^{-1}\frac{-Zs}{(X_{Lm}(\varphi) - Xs)^2 + Y_{Lm}(\varphi)^2 + Zs^2}$$

$$\Theta_{max}(\varphi) = \cos^{-1}\frac{Z_L - Zs}{(X_{Lm}(\varphi) - Xs)^2 + Y_{Lm}(\varphi)^2 + Zs^2}$$

Where:

$$X_{Lm}(\varphi) = X_L + (Xs - Y_L)\cos\varphi^2 + (Y_L)(\cos\varphi \operatorname{sen}\varphi) - \operatorname{sen}\varphi\sqrt{(R_L{}^2 - (Y_L \operatorname{sen}\varphi + (}$$

$$Y_{Lm}(\varphi) = (Y_L)\cos\varphi^2 - (Xs - X_L)(\cos\varphi \operatorname{sen}\varphi) - \cos\varphi\sqrt{(R_L{}^2 - (Y_L \operatorname{sen}\varphi + (Xs - X_L}$$

Where: X_L, Y_L and Z_L, are the coordinates of the points located on the surface of the lamp. Xs, Ys and Zs are the coordinates of the points located on the surface of the films.

5.2. Integration Limits of Eq. 23 of main text

$$\varphi_{min} = \tan^{-1}\left(\frac{X_L - X_{susp}}{Y_L - Y_{susp}}\right) - \sin^{-1}\left(\frac{R_L}{(X_L - X_{susp})^2 + (Y_L - Y_{susp})^2}\right)$$

$$\varphi_{max} = \tan^{-1}\left(\frac{X_L - X_{susp}}{Y_L - Y_{susp}}\right) + \sin^{-1}\left(\frac{RL}{(X_L - X_{susp})^2 + (Y_L - Y_{susp})^2}\right)$$

$$\Theta_{min}(\varphi) = \cos^{-1}\frac{-Z_{susp}}{(X_{Ls}(\varphi) - X_{susp})^2 + (Y_{Ls}(\varphi) - Y_{susp})^2 + Z_s^{\ 2}}$$

$$\Theta_{max}(\varphi) = \cos^{-1}\frac{Z_L - Z_{susp}}{(X_{Ls}(\varphi) - X_{susp})^2 + (Y_{Ls}(\varphi) - Y_{susp})^2 + Z_s^{\ 2}}$$

Where:

$$X_{Ls}(\varphi) = X_L + (X_{susp} - Y_L)\cos\varphi^2 + (Y_L - Y_{susp})(\cos\varphi \operatorname{sen}\varphi) - \operatorname{sen}\varphi\sqrt{(R_L^{\ 2} - (X_s$$

$$Y_{Ls}(\varphi) = Ys_i + (Y_L - Y_{susp})\cos\varphi^2 + (X_{susp} - X_L)(\cos\varphi \operatorname{sen}\varphi) - \cos\varphi\sqrt{(R_L^{\ 2} - (X$$

Where: X_L, Y_L and Z_L, are the coordinates of the points located on the surface of the lamp. X_{susp}, $Y_{susp}$and Z_{susp} are the coordinates of the points evaluated in the suspension volume.

6.- Infrared Spectroscopy

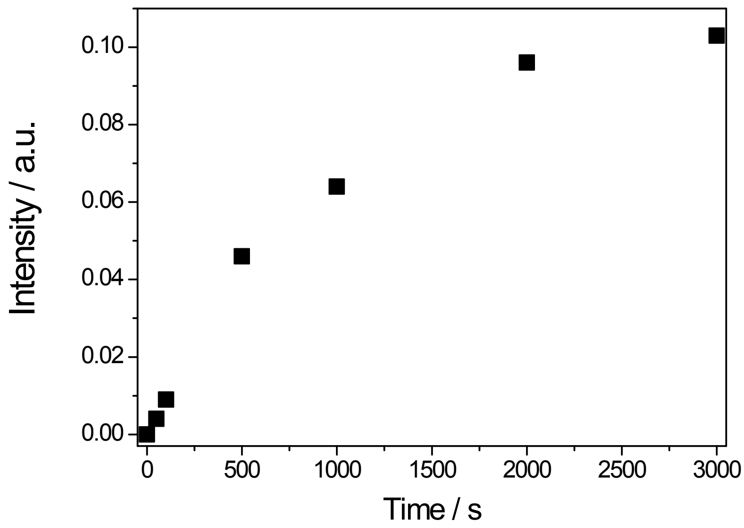

Fig. S5. 1575 cm^{-1} IR band intensity temporal behaviour.

All bands evolving from t = 0 s in the middle panel of Fig. 2 of the main article display the same temporal behaviour of the band presented in Fig. S5 and associated to formate species.